Journal of Sound and Vibration (2002) **254**(5), 911–926
doi:10.1006/jsvi.2001.4135, available online at http://www.idealibrary.com on IDEAL®

VIBRATIONS OF NON-UNIFORM CONTINUOUS BEAMS UNDER MOVING LOADS

Y. A. Dugush and M. Eisenberger

Faculty of Civil Engineering, Technion-Israel Institute of Technology, Technion City, Haifa 32000, *Israel. E-mail: cvrmosh@tx.technion.ac.il*

(*Received* 3 *April* 2001, *and in final form* 10 *September* 2001)

The dynamic behavior of multi-span non-uniform beams transversed by a moving load at a constant and variable velocity is investigated. The continuous beam is modelled using Bernoulli–Euler beam theory. The solution is obtained by using both the modal analysis method and the direct integration method. The natural frequencies and mode shapes used in the solution of this problem are obtained exactly by deriving the exact dynamic stiffness matrices for any polynomial variation of the cross-section along the beam using the exact element method. The mode shapes are expressed as infinite polynomial series. Using the exact mode shapes yields the exact solution for general variation of the beam section in case of constant and variable velocity. Numerical examples are presented in order to demonstrate the accuracy and the effectiveness of the present study, and the results are compared to previously published results.

1. INTRODUCTION

The dynamic behavior of beam structures under moving loads can now be investigated using the exact element method [1] although it has been a topic of interest for well over a century, the time of erection of the early railway bridges. This makes this problem one of the original problems of structural dynamics. Fryba [2] presented in his book analytical solutions for simple problems of simply supported and continuous beams with uniform cross-section. Wu and Dai [3] used the transfer matrix method to determine the natural frequencies and the mode shapes of the continuous beam, and the application of modal analysis to derive the dynamic equations. Lee [4] analyzed the problem by using the assumed-mode method where the intermediate supports of the uniform continuous beam were modelled as linear springs with large stiffness. Henchi *et al.* [5] derived the exact frequencies and mode shapes of a uniform continuous beam by using the dynamic stiffness element method under the framework of finite element approximation. The modal analysis method was applied later to derive the equation of motion. Gutierrez and Laura [6, 7] used simple polynomial terms as the assumed mode, in order to determine the dynamic response of a single span non-uniform beam with various boundary conditions, and loaded by constant and variable moving loads. Zheng *et al.* [8] analyzed the vibration of a multi-span non-uniform beam using the modified beam vibration functions as assumed modes and Hamilton's principle. Ichikawa *et al.* [9] presented a solution for a uniform continuous Euler beam under a concentrated load moving at variable velocity. The solution was achieved by using the mode superposition method. The mode shapes and the natural

0022-460X/02/$35.00

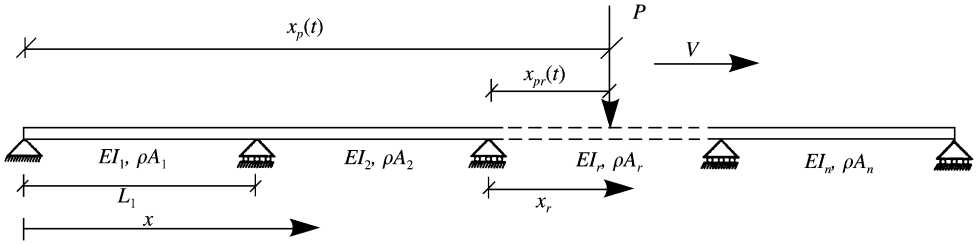

Figure 1. Continuous beam under a single moving load.

frequencies were derived exactly, and the resulting equations of motion in the case of variable velocity were solved numerically using the central difference method. Zhu and Law [10] analyzed a non-uniform continuous Euler beam using Hamilton's principle and the eigen pairs.

In the present study, the exact mode shape and natural frequencies are derived. The modal analysis in combination with integral transformation methods were applied to determine the dynamic deflection of the beam under moving loads. Several examples are given for constant and accelerating moving loads on multi-span non-uniform beams.

2. FORMULATION

The governing differential equation of the non-uniform continuous Euler–Bernoulli beam under concentrated moving load shown in Figure 1 is

$$\frac{\partial^2}{\partial x^2}\left(EI(x)\frac{\partial^2 w(x,t)}{\partial x^2}\right)+\rho A(x)\frac{\partial^2 w(x,t)}{\partial t^2}=P\delta(x-x_p(t)), \tag{1}$$

where $w(x, t)$ is the vertical displacement of the beam. The flexural rigidity of the beam is defined as

$$EI(x)=\sum_{r=1}^{n_{span}} EI_r\left(x-\sum_{i=1}^{r-1}L_i\right)\left(\mathrm{H}\left(x-\sum_{i=1}^{r-1}L_i\right)-\mathrm{H}\left(x-\sum_{i=1}^{r}L_i\right)\right) \tag{2}$$

with $EI_r(x_r)=R_r(x_r)$ being the variable flexural stiffness of the rth span of the beam, and

$$A(x)=\sum_{r=1}^{n_{span}} A_r\left(x-\sum_{i=1}^{r-1}L_i\right)\left(\mathrm{H}\left(x-\sum_{i=1}^{r-1}L_i\right)-\mathrm{H}\left(x-\sum_{i=1}^{r}L_i\right)\right) \tag{3}$$

with $A_r(x_r)$ being the variable area of beam cross-section of the rth span, and $\mathrm{H}(x)$ is the Heaviside function. The variables x_r and t_r are the local distance and time co-ordinate, respectively, measured from the left end of the rth span. $x_{pr}(t)$ is the load position measured from the left end of the rth span, and x and t are the global distance and time co-ordinate, respectively, measured from the left end of the beam. $x_p(t)$ is the load position measured from the left end of beam, P is the magnitude of the concentrated moving load, δ the Dirac delta function, ρ is the beam mass density, and v is the velocity of the moving load.

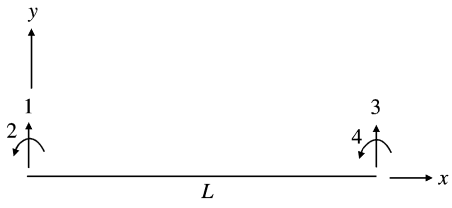

Figure 2. Beam element and degrees of freedom.

2.1. FREE VIBRATION

The free vibration analysis is carried out using the exact element method [1] and the dynamic stiffness method. The governing differential equation of a typical beam element shown in Figure 2 is

$$\partial^2/\partial x^2\ (R(x)\ \partial^2 w(x,t)/\partial x^2) = -\rho A(x)\,\partial^2 w(x,t)/\partial t^2. \tag{4}$$

For polynomial variation of $A(x)$ and $R(x)$ along the element one can write

$$A(x) = \sum_{i=0}^{nA} A_i x^i, \qquad EI(x) = R(x) = \sum_{i=0}^{nR} R_i x^i, \tag{5, 6}$$

introducing a new dimensionless local variable ξ as

$$\xi = x/L. \tag{7}$$

In harmonic vibrations with frequency ω the solution of equation (1) is assumed to be of the form

$$w(x,t) = y(x)\sin(\omega t) \tag{8}$$

and then substituting equations (5–7) into equation (4), yields

$$(\mathrm{d}^2/\mathrm{d}\xi^2)(r(\xi)\,\mathrm{d}^2 y(\xi)/\mathrm{d}\xi^2) - \mathrm{d}(\xi)y(\xi) = 0, \tag{9}$$

where

$$r(\xi) = \sum_{i=0}^{nR} R_i L^i \xi^i, \qquad \mathrm{d}(\xi) = \sum_{i=0}^{nA} \omega^2 \rho A_i L^{i+4} \xi^i = \sum_{i=0}^{nA} \mathrm{d}_i \xi^i. \tag{10, 11}$$

Now the solution $y(\xi)$ is assumed to be an infinite power series

$$y(\xi) = \sum_{i=0}^{\infty} y_i \xi^i. \tag{12}$$

Calculating all the derivatives and substituting the polynomial expressions into equation (9),

$$0 = \sum_{i=0}^{\infty} \sum_{k=0}^{i} \frac{(k+1)(k+2)(i-k+2)!}{(i-k)!}\, r_{k+2} y_{i-k+2} \xi^i$$

$$+\sum_{i=0}^{\infty}\sum_{k=0}^{i}\frac{2(k+1)(i-k+3)!}{(i-k)!}r_{k+1}y_{i-k+3}\xi^i$$

$$+\sum_{i=0}^{\infty}\sum_{k=0}^{i}\frac{(i-k+4)!}{(i-k)!}r_k y_{i-k+4}\xi^i-\sum_{i=0}^{\infty}\sum_{i=0}^{\infty}d_k y_{i-k}\xi^i. \tag{13}$$

To satisfy this equation for every value of ξ, one must have

$$0=\sum_{k=0}^{i}\frac{(k+1)(k+2)(i-k+2)!}{(i-k)!}r_{k+2}y_{i-k+2}$$

$$+\sum_{k=0}^{i}\frac{2(k+1)(i-k+3)!}{(i-k)!}r_{k+1}y_{i-k+3}$$

$$+\sum_{k=0}^{i}\frac{(i-k+4)!}{(i-k)!}r_k y_{i-k+4}-\sum_{k=0}^{i}d_k y_{i-k} \tag{14}$$

or

$$y_{i+4}=1/(i+1)(i+2)(i+3)(i+4)r_0$$

$$\times\left[\sum_{k=0}^{i}d_k y_{i-k}-\sum_{k=0}^{i}\frac{(k+1)(k+2)(i-k+2)!}{(i-k)!}r_{k+2}y_{i-k+2}\right.$$

$$\left.-\sum_{k=0}^{i}\frac{2(k+1)(i-k+3)!}{(i-k)!}r_{k+1}y_{i-k+3}-\sum_{k=1}^{i}\frac{(i-k+4)!}{(i-k)!}r_k y_{i-k+4}\right]. \tag{15}$$

One has all the y_i terms except the first four, which can be found using the boundary conditions. The terms for $y_{i+4}\to 0$ as $i\to\infty$. At $\xi=0$, one has

$$y_0=y(\xi=0),\quad y_1=y'(\xi=0). \tag{16}$$

The terms y_2, y_3 are found from the right end boundary conditions of the element as follows: all of the y_i are linearly dependent on the first two, and they are functions of the coefficients in $r(\xi)$ and ω. The terms of the element dynamic stiffness matrix can be found directly from the derivatives of the shape function. The terms in the stiffness matrix are defined as the holding actions at both ends of the beam, due to unit translation or rotation, at each of the four degrees of freedom, one at a time. Thus, there are four sets of boundary conditions

$$Y_1(0)=1,\quad Y_1'(0)=Y_1(L)=Y_1'(L)=0,\quad Y_2'(0)=1,\quad Y_2(0)=Y_2(L)=Y_2'(L)=0,$$

$$Y_3(L)=1,\quad Y_3'(L)=Y_3(0)=Y_3'(0)=0,\quad Y_4'(L)=1,\quad Y_4(L)=Y_4(0)=Y_4'(0)=0. \tag{17}$$

There are four shape functions, corresponding to these four sets, resulting in the holding actions

$$V(0)=(r(0)/L^3)\,\mathrm{d}^3Y_i/\mathrm{d}\xi^3+(1/L^3)\,(\mathrm{d}r(0)/\mathrm{d}\xi)\,\mathrm{d}^2Y_i/\mathrm{d}\xi^2,\qquad M(0)=-(r(0)/L^2)(\mathrm{d}^2Y_i/\mathrm{d}\xi^2), \tag{18, 19}$$

$$V(1) = -(r(1)/L^3)(\mathrm{d}^3 Y_i/\mathrm{d}\xi^3) - (1/L^3)(\mathrm{d}r(1)/\mathrm{d}\xi)(\mathrm{d}^2 Y_i/\mathrm{d}\xi^2), \qquad M(1) = (r(1)/L^2)\,\mathrm{d}^2 Y_i/\mathrm{d}\xi^2, \tag{20, 21}$$

where V is the shear force and M is the moment. The ith column of element stiffness matrix will be

$$Kd(1, i) = (6R(0)/L^3)\,Y_{i,3} + (2R'(0)/L^2)\,Y_{i,2}, \qquad Kd(2, i) = -(2R(0)/L^2)\,Y_{i,2}, \tag{22, 23}$$

$$Kd(3, i) = -\frac{R(L)}{L^3}\sum_{k=3}^{\infty} k(k-1)(k-2)Y_{i,k} - \frac{R'(L)}{L^2}\sum_{k=2}^{\infty} k(k-1)Y_{i,k}, \tag{24}$$

$$Kd(4, i) = \frac{R(L)}{L^2}\sum_{k=2}^{\infty} k\,(k-1)Y_{i,k}. \tag{25}$$

Once one obtains the dynamic stiffness matrices of all beam elements for a given ω, the global stiffness matrix of the continuous beam is assembled as in the finite element method. The natural frequencies are the values of ω that cause the global stiffness matrix to become singular. These natural frequencies are obtained by using an ordinary bisection method for finding the values of the frequency that cause the determinant of the global stiffness matrix to become zero. Giving a value to one of the beam free degrees of freedom and computing the rest and multiplying these values with suitable element exact shape functions yields the exact mode shapes as infinite power series

$$\phi_{jr}(x_r) = \sum_{i=1}^{4} y_{ir}(x_r, \omega_j)d_{jr}^i = \sum_{j=1}^{\infty} \varphi_j x_r^j, \tag{26}$$

where $\phi_{jr}(x_r)$ is the jth mode shape at the rth span, $y_{ir}(x_r, \omega_j)$ is the ith shape function of the rth element for the jth natural frequency, and d_{jr}^i is the ith degree of freedom at the rth element end in the jth mode shape.

The complete shape function j of the beam is obtained as

$$\Phi_j(x) = \sum_{r=1}^{n_{span}} \phi_{jr}\left(x - \sum_{i=1}^{r-1} L_i\right)\left(\mathrm{H}\left(x - \sum_{i=1}^{r-1} L_i\right) - \mathrm{H}\left(x - \sum_{i=1}^{r} L_i\right)\right). \tag{27}$$

2.2. FORCED VIBRATION

The solution of equation (1) is obtained using the methods of modal superposition in combination with direct integration. One assumes the vertical displacement of the beam to be of the form

$$w(x, t) \cong \sum_{j=1}^{n_{mode}} Q_j(t)\Phi_j(x), \tag{28}$$

where $Q_j(t)$ is the jth total unknown time function, and n_{mode} is the number of participating modes. Substituting equation (28) into equation (1), and multiplying with each of the

participating mode shapes $\Phi_k(x)$, $k = 1, \ldots, n_{mode}$, and integrating, one has

$$\int_0^L \sum_{j=1}^{n_{mode}} \Phi_j''''(x) EI(x) \Phi_k(x) Q_j(t)\, \mathrm{d}x + \int_0^L \sum_{j=1}^{n_{mode}} \Phi_j(x) \rho A(x) \Phi_k(x) \ddot{Q}_j(t)\, \mathrm{d}x$$

$$= \int_0^L P\delta(x - x_p(t)) \Phi_k(x)\, \mathrm{d}x. \tag{29}$$

The generalized stiffness and mass of the beam are

$$k_{jk} = \int_0^L \Phi_j''(x) EI(x) \Phi_k''(x)\, \mathrm{d}x, \qquad m_{jk} = \int_0^L \Phi_j(x) \rho A(x) \Phi_k(x)\, \mathrm{d}x \tag{30}$$

and from the orthogonality of the exact mode shapes

$$k_{jk} = m_{jk} = 0 \tag{31}$$

for $j \neq k$, and when $j = k$ for j, $k = 1, \ldots, n_{mode}$

$$k_j = \sum_{r=1}^{n_{span}} \int_0^{L_r} \phi_{jr}''(x_r) EI_r(x_r) \phi_{jr}''(x_r)\, \mathrm{d}x_r, \qquad m_j = \sum_{r=1}^{n_{span}} \int_0^{L_r} \phi_{jr}(x_r) \rho A_r(x_r) \phi_{jr}(x_r)\, \mathrm{d}x_r. \tag{32}$$

The jth natural frequency of the continuous beam is

$$\omega_j = \sqrt{k_j / m_j}. \tag{33}$$

Substituting terms of equations (32, 33) into equation (29) using the Dirac function properties to obtain the jth equation of motion of the form

$$\ddot{Q}_j(t) + \omega_j^2 Q_j(t) = (P/m_j) \Phi_j(x = x_p(t)) \tag{34}$$

or for each span r one can write

$$\ddot{q}_{jr}(t) + \omega_j^2 q_{jr}(t) = (P/m_j) \phi_{jr}(x_r = x_{pr}(t)), \tag{35}$$

where

$$Q_j(t) = \sum_{r=1}^{n_{span}} q_{jr}\left(t - \sum_{i=1}^{r-1} T_i\right)\left(\mathrm{H}\left(t - \sum_{i=1}^{r-1} T_i\right) - \mathrm{H}\left(t - \sum_{i=1}^{r} T_i\right)\right) \tag{36}$$

and T_i is the time required for the load to transverse the length of the ith span. Considering a linearly varying velocity of the load, one can write for span r

$$v_r(t_r) = v_{0r} + a t_r, \tag{37}$$

where v_{0r} is the initial velocity at the rth span left end, and a is the constant acceleration. The load position from the left end of the rth span is

$$x_{pr}(t_r) = v_{0r} t_r + \tfrac{1}{2} a t_r^2 \tag{38}$$

and in this case the left side of equation (35) is of the form

$$\frac{P}{m_j}\phi_{jr}(x_r = x_{pr}(t_r)) = \frac{P}{m_j}\sum_{i=0}^{\infty}\varphi_i(v_{0r}t_r + \tfrac{1}{2}at_r^2)^i. \tag{39}$$

The resulting equation of motion can be solved analytically using the method of the Laplace–Carson integral transformation. Here, a different solution is presented based on the "exact element method" technique. The term in equation (39) can be expanded and each mode equation of motion can have the form

$$\ddot{q}_r(\tau_r) + \omega_r^2 q_r(\tau_r) = p(\tau_r), \tag{40}$$

where

$$p(\tau_r) = \sum_{i=0}^{n_p} p_i \tau_r^i \tag{41}$$

and τ_r is the dimensionless time co-ordinate of the rth span expressed as

$$\tau_r = t_r/T_r, \text{ and } \omega_r = \omega T_r. \tag{42, 43}$$

The initial conditions of the beam are

$$q_1(0) = \delta_0, \quad \dot{q}_1(0) = \vartheta_0 \tag{44}$$

and the continuity conditions between the rth span and $r + 1$ span is

$$q_{r+1}(\tau_{r+1} = 0) = q_r(\tau_r = 1), \qquad \dot{q}_{r+1}(\tau_{r+1} = 0) = (T_{r+1}/T_r)\,\dot{q}_r(\tau_r = 1). \tag{45, 46}$$

According to the exact element technique the solution of equation (40) is of the form

$$q(\tau) = \sum_{i=0}^{\infty}\theta_i\tau^i. \tag{47}$$

Substituting equations (41) and (47) into equation (40), one finally reaches the recurrence formula

$$\theta_{i+2} = (p_i - \omega^2\theta_i)/(i+1)(i+2), \tag{48}$$

where the first two θ_i terms are found directly from the initial conditions

$$\theta_0 = q(0), \quad \theta_1 = \dot{q}(0). \tag{49}$$

From the recurrence formula one can find the unknown time function terms of any desired accuracy.

3. EXAMPLES

3.1. EXAMPLE 1: THREE EQUAL-SPAN STEPPED BEAM UNDER A SINGLE CONCENTRATED MOVING LOAD

The first example is of a beam with three equal spans (see Figure 3), with a uniform section at each span, and the central span has a double flexural stiffness. Each span length is

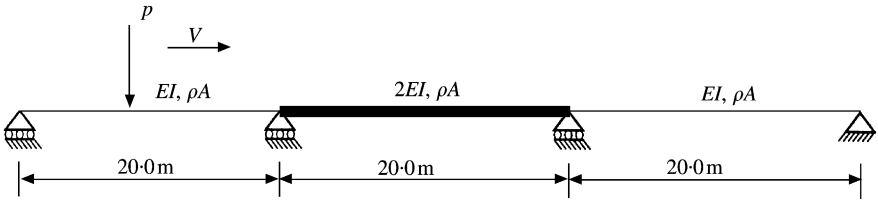

Figure 3. Three-span stepped beam under a single concentrated moving load.

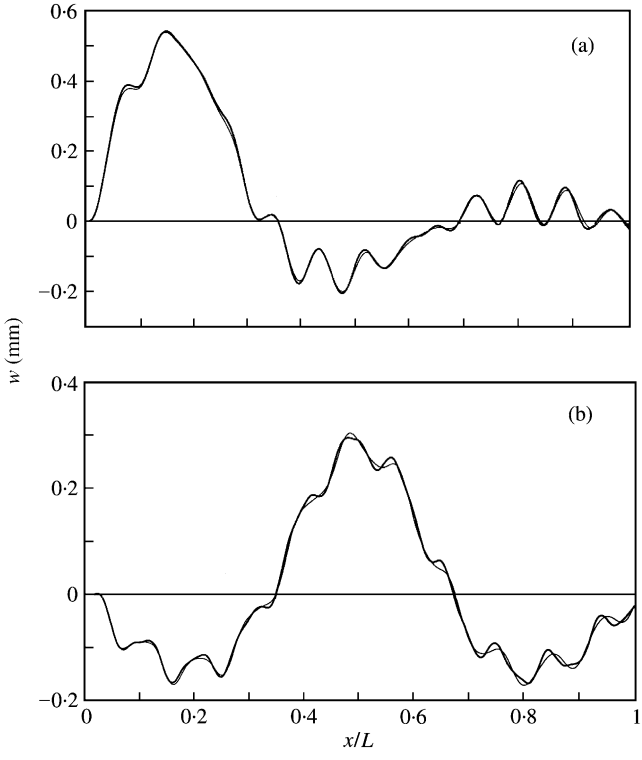

Figure 4. Deflections at midspan positions of (a) the first and (b) central spans: ——, present study results; ——, reference [8] results.

20·0 m, the magnitude of the concentrated load is $P = 9{\cdot}8$ kN, moving at $v = 34$ m/s, the beam mass per unit length is $\rho A = 1000$ kg/m, and the flexural stiffness of the side spans is $EI = 1{\cdot}96 \times 10^6$ kN m^2. The solution of the problem was performed using the first five mode shapes. The exact natural frequencies corresponding to these mode shapes are 38·98227, 47·63379, 75·23519, 152·09888 and 166·12375 rad/s. The dynamic response at midpoint locations of the first and second spans are shown in Figure 4. The results of reference [8] were attached to the present study results, and very good agreement is observed.

3.2. EXAMPLE 2: THREE-SPAN HAUNCHED BEAM UNDER A SINGLE CONCENTRATED MOVING LOAD

For the second example a three-span continuous beam shown in Figure 5 was solved. The beam has linearly varying depth at the interior supports and is loaded by a single

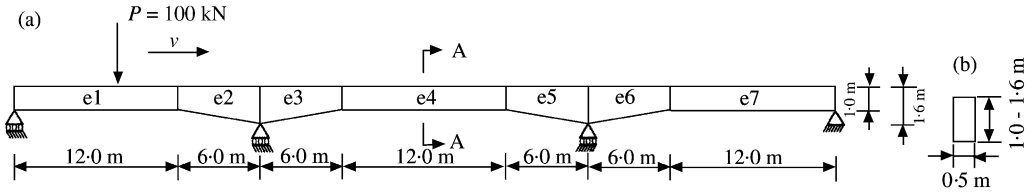

Figure 5. A three-span continuous haunched beam under a single moving load: (a) elevation; (b) section A–A.

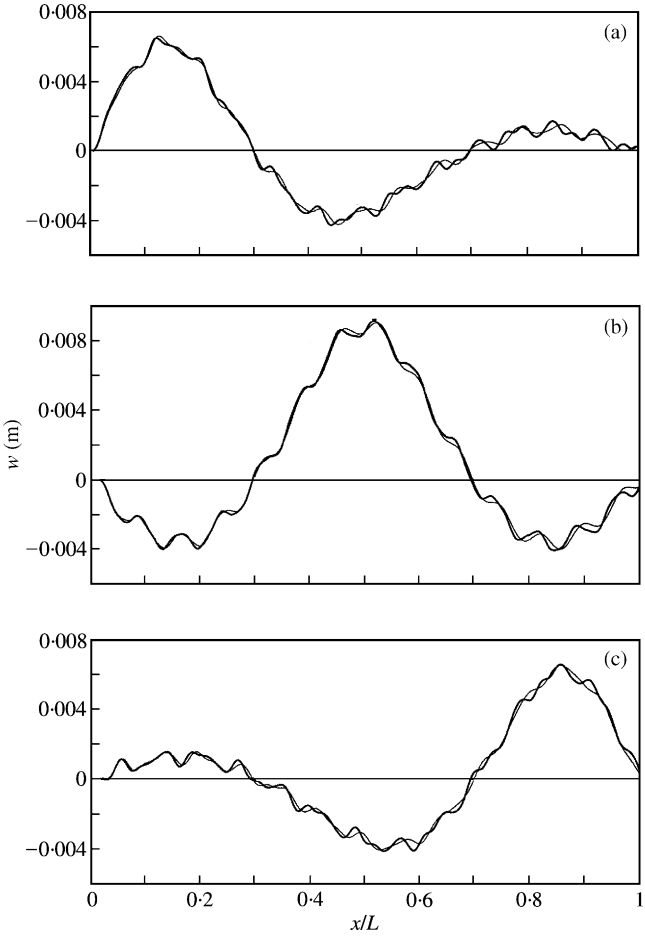

Figure 6. Deflections at midspan positions of (a) the first, (b) second and (c) third spans: ——, present study results; ——, reference [8] results.

concentrated constant load $P = 100$ kN moving at $v = 17$ m/s. The modulus of elasticity and mass density of the beam is 3×10^{10} N/m^2 and 2400 kg/m^3 respectively. The problem was solved by dividing the beam into seven elements, one element in each region ($e1, \ldots, e7$), using the five exact mode shapes: 24·62893, 41·83935, 58·04443, 99·45083, and 144·15530 rad/s. The dynamic response of the midpoint positions of the three spans is shown in Figure 6. The results of reference [8] are attached to the present study results for comparison, showing good agreement.

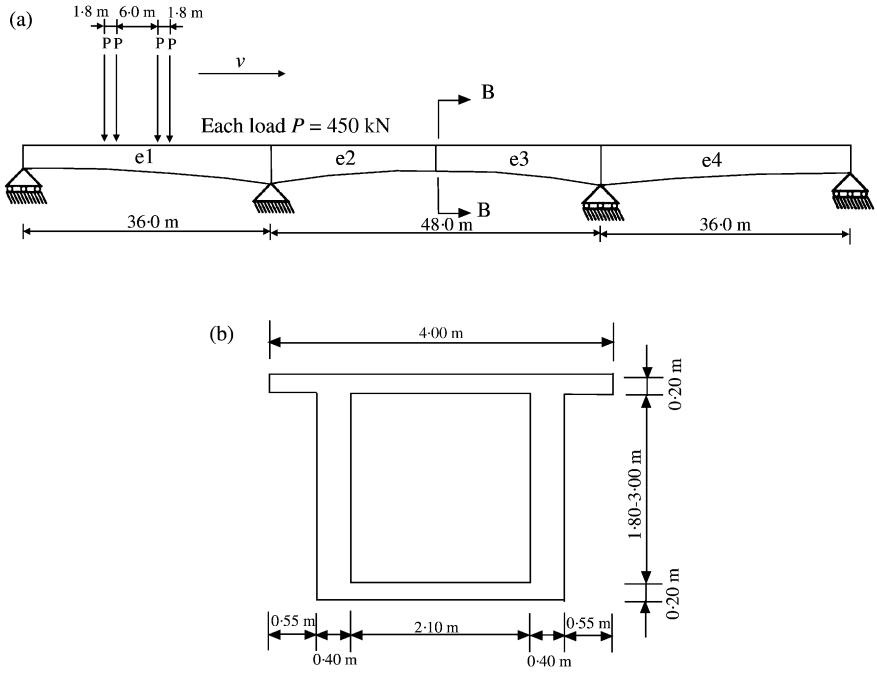

Figure 7. A three-span continuous bridge with parabolic soffit under a moving vehicle of four axles: (a) elevation; (b) section B–B.

3.3. EXAMPLE 3: THREE-SPAN BOX BRIDGE OF PARABOLIC SOFFIT UNDER A MOVING VEHICLE OF FOUR AXLES

The three-span continuous bridge shown in Figure 7 with a total length of 120·0 m and a box cross-section with parabolically varying depth, carrying a vehicle of four axles moving at a constant velocity, is analyzed. Each axle is 450 kN, the modulus of elasticity of the beam $E = 3 \times 10^{10}\,\mathrm{N/m^2}$ and the density $\rho = 2400\,\mathrm{kg/m^3}$. The beam was divided into four elements ($e1, \ldots, e4$), only one element for the side spans and two elements for the central one. The cross-sectional area is a second order polynomial, and the flexural stiffness is a rational function replaced by an interpolation polynomial of the sixth degree which is a very accurate approximation of the original function. The first eight natural frequencies of the bridge are: 18·15905, 29·92832, 38·70981, 70·76431, 104·81149, 116·79492, 154·37644, and 220·51267 rad/s, and the corresponding mode shapes are shown in Figure 8. The dynamic response of the bridge was performed considering only one axle and the total response of the vehicle was achieved by superposition.

A convergence study was carried out for this example. The contribution of the first 10 modes to the deflection at the center of the first and second spans, whilst the vehicle center was over the first and the second spans, for various speeds, are shown in Tables 1 and 2 respectively. It can be observed that the first five modes are sufficient to evaluate the displacement. D_d is the displacement amplification factor. The development of the exact mode shapes enables one to obtain the dynamic internal forces by deriving these mode shapes. The dynamic bending moments are obtained from

$$M(x, t) = -EI(x)\,\partial^2 w(x, t)/\partial x^2. \tag{50}$$

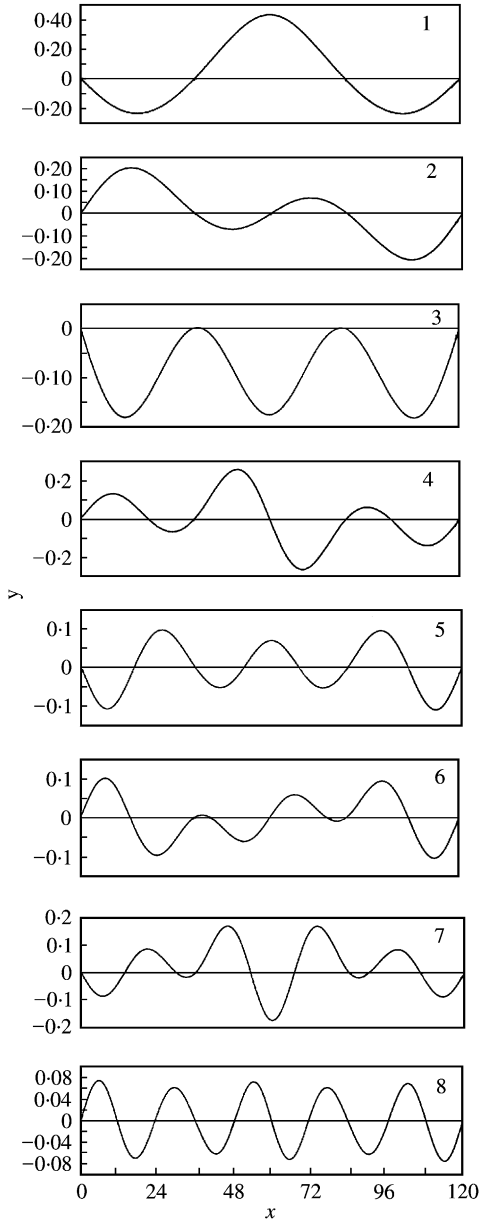

Figure 8. Eight first mode shapes of the bridge with the parabolic soffit.

The contribution of the first 15 mode shapes to the moment at the center of the first span, and at the first internal support, while the vehicle was at the center of the first span for various speeds are shown in Tables 3 and 4 respectively. D_m is the moment amplification factor. The displacement at the midpoint position of the three spans for a vehicle speed of 17 m/s using 5 mode shapes is shown in Figure 9, together with the results from reference [8], and a good agreement is observed. The dynamic bending moment at the center of the first span and at the first interior support using 5, 10, and 15 mode shapes are presented in Figures 10 and 11 respectively. It can be observed that the first 10 modes are sufficient to

TABLE 1

The contribution of each mode to the deflection (mm) at the center of the first span, while the vehicle center is at the center of the first span

Mode no. (i)	Speed (v) (m/s)				
	~ 0	17	56	100	125
1	6·24	6·34	6·96	8·58	7·21
2	6·62	6·63	6·69	8·12	9·86
3	2·87	2·89	2·87	3·00	3·48
4	0·07	0·08	0·08	0·08	0·06
5	0·02	0·02	0·02	0·02	0·01
6	0·05	0·05	0·05	0·05	0·08
7	0·04	0·04	0·04	0·04	0·04
8	0·04	0·04	0·05	0·05	0·04
9	0·04	0·04	0·04	0·04	0·04
10	0·01	0·01	0·01	0·01	0·01
Σ	16·00	16·13	16·81	19·99	20·83
D_d	1·000	1·008	1·051	1·249	1·302

TABLE 2

The contribution of each mode to the deflection (mm) at the center of the second span, while the vehicle center is at the center of the second span

Mode no. (i)	Speed (v) (m/s)				
	~ 0	17	56	100	125
1	22·59	22·39	24·52	20·89	33·68
2	0·00	0·00	0·00	0·00	0·00
3	3·12	3·20	2·92	3·41	3·65
4	0·00	0·00	0·00	0·00	0·00
5	0·18	0·18	0·18	0·18	0·19
6	0·00	0·00	0·00	0·00	0·00
7	0·22	0·22	0·22	0·23	0·23
8	0·00	0·00	0·00	0·00	0·00
9	0·01	0·01	0·01	0·01	0·01
10	0·00	0·00	0·00	0·00	0·00
Σ	26·12	26·00	27·85	24·72	37·76
D_d	1·000	0·995	1·066	0·946	1·446

evaluate the bending moments of the bridge. The curves in Figures 9–11 are not smooth. They represent the effect of the velocity, and for higher speeds the curves become less dependent on the higher frequencies of the beam. For lower speeds the response is oscillating around the static solution for the particular beam.

3.4. EXAMPLE 4: THREE-SPAN STEPPED BEAM UNDER AN ACCELERATING SINGLE MOVING LOAD

In this example, the beam presented in Example 1 (Figure 3), with the following normalized dimensions, $L = 3{\cdot}0$, $\rho A = 1{\cdot}0$, $EI = 1{\cdot}0$, and $P = 1{\cdot}0$, was analyzed. The

TABLE 3

The contribution of each mode to the moment (kNm) at the center of the first span, while the vehicle center is at the center of the first span

Mode no. (i)	Speed (v) (m/s)				
	~0	17	56	100	125
1	3331·4	3385·8	3713·2	4577·7	3846·9
2	3888·4	3899·2	3929·1	4772·1	5792·5
3	1829·6	1838·8	1830·2	1917·5	2222·0
4	49·7	51·3	51·0	54·5	37·5
5	58·9	55·1	57·6	60·8	19·9
6	159·5	159·5	158·6	155·7	234·0
7	132·1	132·1	130·1	137·6	135·2
8	217·1	217·1	240·5	229·7	216·5
9	210·8	205·5	218·7	199·1	216·5
10	50·9	50·3	51·3	46·9	58·3
11	−0·1	−0·3	1·0	−0·1	0·4
12	7·9	6·1	15·0	17·4	8·4
13	8·3	7·9	6·7	9·2	11·4
14	−2·7	−2·4	−4·0	−2·6	−4·7
15	−21·7	−20·8	−15·9	−26·1	−21·3
Σ	9920·1	9985·2	10383·1	12149·4	12773·5
D_m	1·000	1·007	1·047	1·225	1·228

TABLE 4

The contribution of each mode to the moment (kNm) at the first interior support, while the vehicle center is at the center of the first span

Mode no. (i)	Speed (v) (m/s)				
	~0	17	56	100	125
1	2635·7	2678·8	2937·8	3621·8	3043·7
2	−3586·1	−3596·0	−3623·6	−4401·1	−5342·2
3	−4398·3	−4420·4	−4399·8	−4609·5	−5341·7
4	−520·4	−537·0	−534·1	−570·5	−392·0
5	−97·6	−91·3	−95·4	−100·7	−33·0
6	−448·7	−453·1	−450·4	−442·2	−664·7
7	−396·4	−397·0	−391·1	−413·7	−406·5
8	−2·5	−2·6	−2·9	−2·7	−2·6
9	271·3	264·4	281·5	256·1	278·6
10	173·3	171·4	174·8	159·7	198·7
11	1·0	2·5	−6·9	0·7	−3·2
12	13·4	10·4	25·6	29·6	14·3
13	21·3	20·1	17·2	23·4	29·0
14	−6·0	−5·4	−8·7	−5·7	−10·4
15	15·5	14·9	11·3	18·3	15·2
Σ	−6324·5	−6340·3	−6064·7	−6435·5	−8616·8
D_m	1·000	1·002	0·959	1·018	1·362

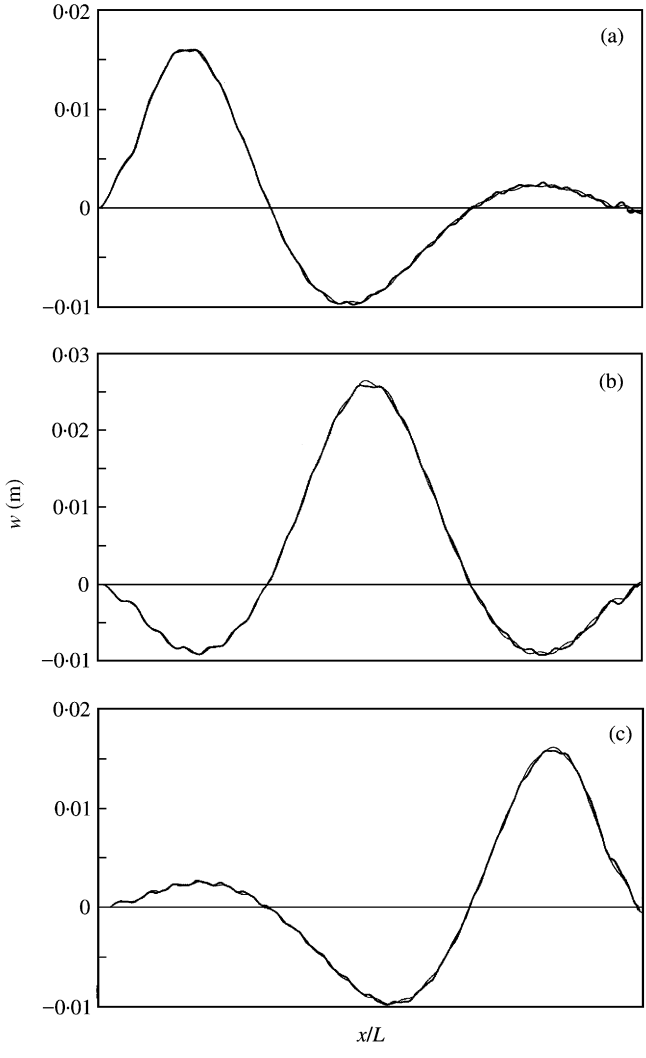

Figure 9. Deflections at midspan positions of (a) span 1, (b) span 2 and (c) span 3 from the arrival of the first axle till the departure of the fourth one: ——, present study results; ——, reference [8] results.

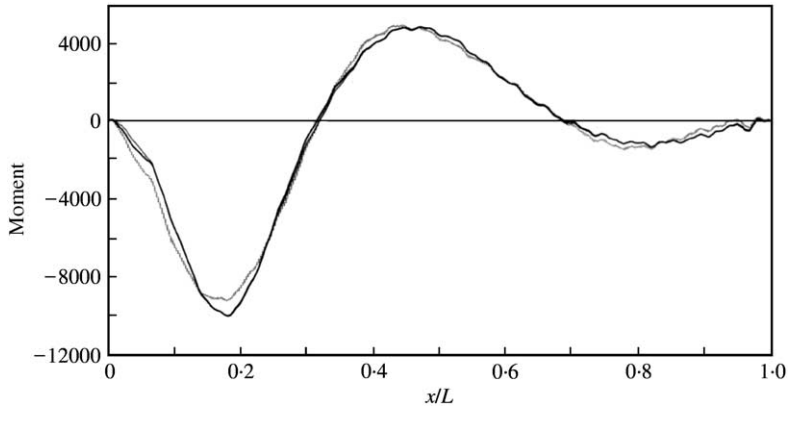

Figure 10. The bending moment (kN m) at the center of the first span using ~~~~~~~~~~, 5; ——, 10; ——, 15 mode shapes.

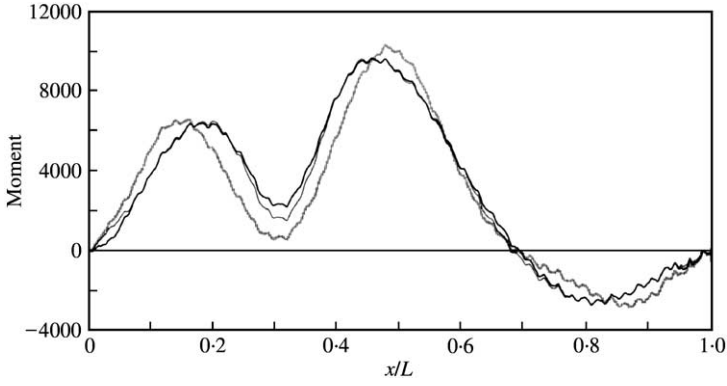

Figure 11. The bending moment (kN m) at the first interior support using ·····, 5; ——, 10; ——, 15 mode shapes.

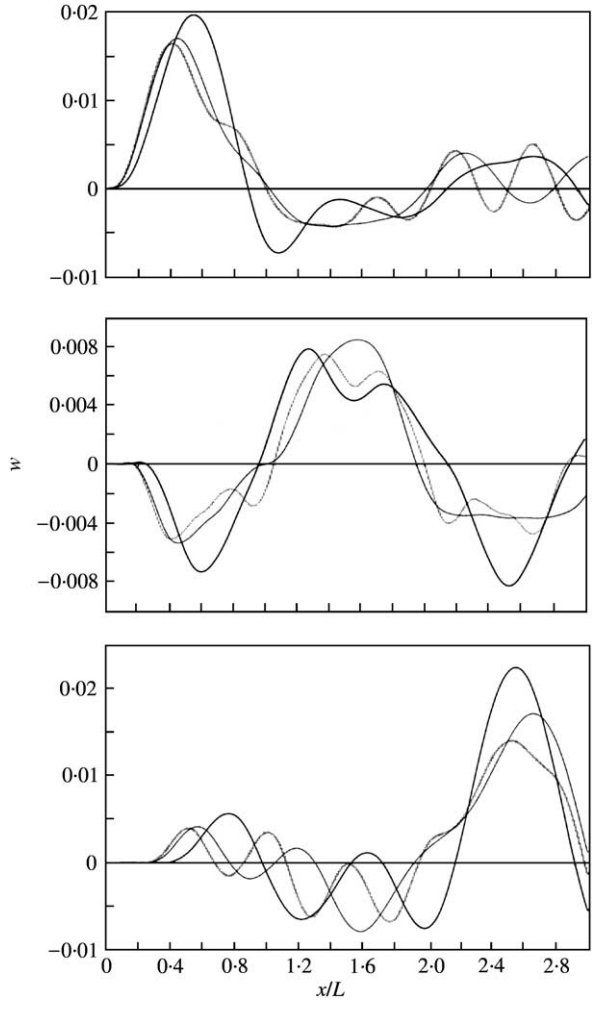

Figure 12. The dynamic deflection at the midpoint of (a) span 1, (b) span 2 and (c) span 3. Key ·····, $a = 0{\cdot}4$, $v_{01} = 1{\cdot}0$; ——, $a = 0$, $v_{01} = 1{\cdot}0$; ——, $a = 0$, $v_{av} = 1{\cdot}483$.

concentrated load is moving at a linearly varying velocity. The initial velocity at the left end of the beam is v_{01}, and the constant acceleration is a.

The solution of the problem was based on the first five mode shapes. The dynamic deflections at the midpoint positions of the three spans are presented in Figure 12 for three cases: (1) initial velocity $v_{01} = 1{\cdot}0$ and acceleration $a = 0{\cdot}4$, (2) constant velocity v_{01}, and (3) for constant velocity of $v_{av} = 1{\cdot}483$, which is the average velocity of the accelerating load. This problem was also presented in reference [9], and it is in good agreement with the present study results.

4. CONCLUSIONS

The dynamic behavior of a non-uniform continuous beam under moving load has been investigated. The natural frequencies and mode shapes of non-uniform continuous beams are obtained exactly. The use of the exact mode shapes yields the exact solution of the moving load problem. The exact mode shapes for non-uniform beams are orthogonal yielding uncoupled equations of motion. This reduces the numerical effort in the solution, and each equation can be solved independently. A smaller number of mode shapes are required to obtain accurate solutions, compared with the number of modes in the assumed mode method. The exact mode shapes are derived in order to find the internal forces. It is demonstrated that for an accurate evaluation of the internal forces, one needs to include more mode shapes than for accurate calculation of the deflections.

ACKNOWLEDGMENTS

F. T. K. Au and the rest of the authors of reference [8] are acknowledged for their contribution and collaboration.

REFERENCES

1. M. Eisenberger 1990 *American Institute of Aeronautics and Astronautics* **28**, 1105–1109. Exact static and dynamic stiffness matrix for general variable cross section members.
2. L. Fryba 1999 *Vibration of Solids and Structures under Moving Loads*. Praha: Academia.
3. J.-S. Wu and C.-W. Dai 1987 *Journal of Structural Engineering* **113**, 458–474. Dynamic responses of multi-span non-uniform beams due to moving loads.
4. H. P. Lee 1994 *Journal of Sound and Vibration* **171**, 361–368. Dynamic response of a beam with intermediate point constraints subject to a moving load.
5. K. Henchi, M. Fafard, G. Dhatt and M. Talbot 1997 *Journal of Sound and Vibration* **199**, 33–50. Dynamic behavior of multi-span beams under moving loads.
6. R. H. Gutierrez and P. A. A. Laura 1996 *Journal of Sound and Vibration* **195**, 353–358. Transverse vibrations of beams traversed by point masses: a general, approximate solution.
7. R. H. Gutierrez and P. A. A. Laura 1997 *Journal of Sound and Vibration* **207**, 419–425. Vibrations of a beam of non-uniform cross-section traversed by a time varying concentrated force.
8. D. Y. Zheng, Y. K. Cheung, F. T. K. Au and Y. S. Cheng 1998 *Journal of Sound and Vibration* **212**, 455–467. Vibration of multi-span non-uniform beams under moving loads by using modified beam vibration functions.
9. M. Ichikawa, A. Matsuda and Y. Miyakawa 1999 *Transactions of the Japan Society for Aeronautical and Spaces Sciences* **41**, 168–173. Simple analysis of a multi-span beam under moving loads with variable velocity.
10. X. Q. Zhu and S. S. Law 2001 *Journal of Sound and Vibration* **240**, 962–970. Precise time-step integration for the dynamic response of a continuous beam under moving loads.